Available online at www.sciencedirect.com

ScienceDirect

Procedia Structural Integrity 5 (2017) 217–224

Structural Integrity Procedia

www.elsevier.com/locate/procedia

2nd International Conference on Structural Integrity, ICSI 2017, 4-7 September 2017, Funchal, Madeira, Portugal

Finite Element Analysis of Crack Growth for Structural Health Monitoring of Mooring Chains using Ultrasonic Guided Waves and Acoustic Emission

Ángela Angulo[a,b]*, Jane Allwright[a], Cristinel Mares[b], Tat-Hean Gan[a,b], Slim Soua[a]

[a]*TWI Ltd, Integrity management Group. Granta Park, Great Abington, Cambridge, CB21 6AL, United Kingdom*
[b]*Brunel University, Kingston Lane, Uxbridge, Middlesex, UB8 3PH, United Kingdom*

Abstract

As offshore oil and gas exploration and production goes further afield and into deeper waters, more offshore operations, are conducted from floating platforms, which are moored to the seabed by chains, polyester tether lines, or combinations of both. Moreover, the forecasted large scale deployment of offshore renewable energy systems in deep water will rely upon similar mooring systems. Mooring lines are safety-critical systems on offshore floating and semi-submersible platforms. The lines are usually subject to immense environmental and structural forces such as currents, oceans waves, and hurricanes. Other forces include impact with the seabed, abrasion, increased drag due to accumulation of marine organisms and salt water corrosion. Failure of one or more of mooring lines can result in disastrous consequences for safety, the environment and production.
Mooring chain life can be significantly reduced, leading to unacceptable risk of catastrophic failure, if early damage is not detected. Chain mounted equipment is available to monitor chain tension and bending, but detection of damage caused by stress concentrations, fatigue, corrosion and fretting or combinations of these is not currently possible. The Ultrasonic Guided Waves (UGW) and Acoustic Emission (AE) techniques are capable of detecting cracks in mooring chains and fatigue damage. This paper describes a methodology of Finite Element Analysis (FEA) for crack initiation and crack growth simulation for Structural Health Monitoring (SHM) applying UGW and AE.

Peer-review under responsibility of the Scientific Committee of ICSI 2017

Keywords: mooring chain, structural integrity, structural health monitoring, acoustic emission, guided wave, crack growth;

* Corresponding author. Tel.: +44-1223-899-091; fax: +44-1223-892-588.
E-mail address: angela.angulo@twi.co.uk

2452-3216
Peer-review under responsibility of the Scientific Committee of ICSI 2017
10.1016/j.prostr.2017.07.119

1. Guided Ultrasonic Waves approach

A Medium Range Ultrasonic Test (MRUT) has been developed for chains that use Ultrasonic Guided Waves (UGW). UGW propagate long distances along elongated objects such as pipes and cylinders, because the multiplying effects of internal reflections from the objects boundaries gives rise to waves that are 'guided' and suffer relatively low energy losses. The wave modes are complex however. The so-called Dispersion Curves (Thompson, 1996) show that as the frequency increases so does the number of wave modes. The additional wave modes increase 'noise' and have the potential to reduce test sensitivity. The high noise due to the presence of multiple UGW modes may be partly compensated with signal processing algorithms that differentiate the higher order modes. Alternatively, instead of relying on one ultrasound frequency in the test, the technique might involve a sweep through a range of test frequencies. Some experimental data has already been derived from chains in this way.

UGW are used in the Long Range Ultrasonic Testing (LRUT) of pipes (Desai, 2011). In LRUT the transmitted wave mode from the transducer tool wrapped around the pipe is symmetrical and either Longitudinal or Torsional. However, around chains, a symmetrical wave will become distorted by the chain curvature (Fig. 1) to become a flexural. The distortion has been studied using numerical models supported by experimentation. Another option is to use Rayleigh waves. These propagate along the surface only and exist at high frequencies when the frequency-thickness product is beyond a certain limit defined by the thickness of the pipe. However Rayleigh waves are likely to be strongly affected by surface roughness (Toigo, 1997).

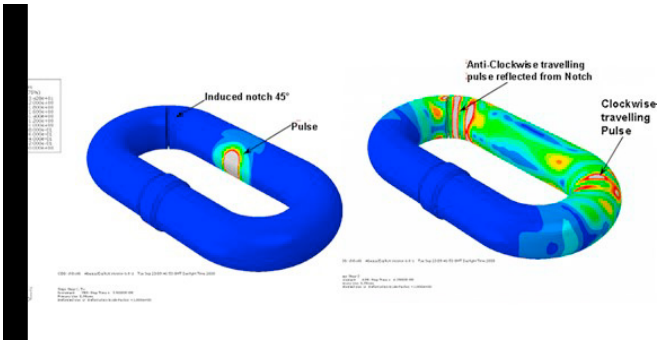

Fig. 1. Distortion of UGW around a chain link.

1.1. Finite element modelling

Finite Element Analysis (FEA) has been used to study the complex UGW propagation around chains and therefore provides a theoretical basis for ultrasound frequency selection for chain links and to aid the optimisation of the inspection technique.

The modelling work was conducting using the commercially available finite element software, Abaqus. The models were linear elastic and assumed the following material properties for carbon manganese steel: Young's modulus = 207GPa, Poisson's ratio = 0.3, Density = 7830kg/m3. A chain link of diameter 110mm was used in the analysis.

The finite element mesh was refined such that there were at least eight elements per wavelength for the smallest possible wavelength in the system. The elements used were 8-node linear bricks. In order to investigate the inspection of chain links, a number of models have been generated as follows.

- Natural frequency extraction models to calculate the dispersion characteristics of the straight section of the chain link. This modelling method (Sanderson, 2002) can be used with most commercial finite element software. It is able to calculate dispersion curves for prismatic structures of any cross-section.
- Transient wave propagation models to calculate the mode conversion that occurs when UGW propagate around the bends in the link.
- Transient wave propagation analyses of the whole link including the weld at a range of UGW frequencies.

1.2. Modelling results

A wave propagation model was used to understand the behavior of UGW as they propagate around the bend in the chain link. One bend was modelled and the ends of the model were elongated to prevent end reflections from interfering with the signals received. A single ring of exciters was used so that the pulse would propagate in both directions.

The magnitude of the displacement after excitation of a 10-cycle 40kHz pulse is shown in Fig. 2. It can be seen that the signal is no longer axisymmetric after propagation around the bend. This indicates mode conversion effect. Analysis was carried out to quantify the wave modes present in the signal after propagation around the bend. A mode filtering technique was used to separate the wave modes by circumferential order (Catton, 2009). Since a torsional excitation was applied, it was assumed that wave modes in the torsional family were present. Fig. 3 shows the amplitudes of the individual wave modes plotted against circumferential order. It can be seen that there is a strong F(1,2) wave mode after passing the bend while T(0,1) wave mode propagates in the other direction along the straight section. The amplitude decreases with increasing circumferential order as would be expected.

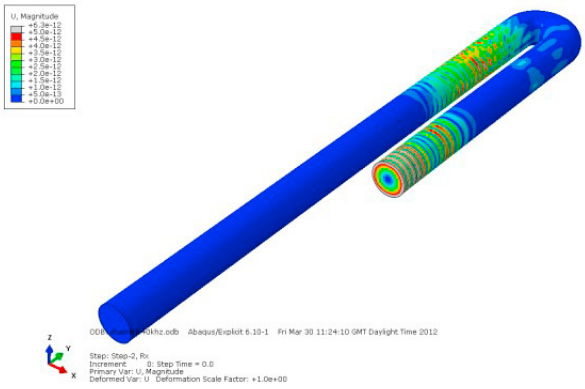

Fig. 2. Displacement magnitude after propagation of a 10-cycle 40kHz pulse around the bend.

Finally, a model of the whole chain link was created and a range of frequencies from 30kHz to 70kHz were analysed. Excitation was applied using two rings to match the experimental work, where phasing is used to remove the wave propagating in one direction while reinforcing the wave propagating in the other. The ring spacing was 30mm and 16 transducers around the circumference were simulated in each ring. The weld was idealised to a triangular shape with a height of 5mm and a length of 60mm on the opposite side of the chain from the ring.

Fig.3. shows the von-Mises stress in the chain link just after the input of a 10-cycle 30kHz pulse. As before, it is clear that significant mode conversion has occurred.

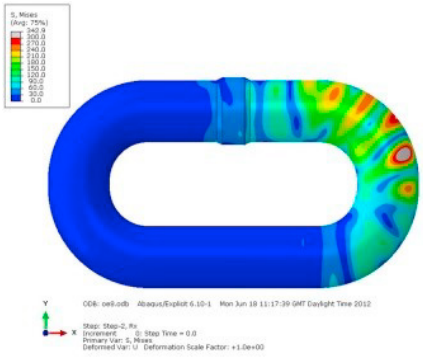

Fig. 3. Von-Mises stress distribution in a chain link just after excitation of a 10-cycle 30kHz pulse.

The mode filtering technique was applied so that the A-scan for individual modes could be assessed. At 30kHz the reflections from the weld were distinct and there is relatively little 'noise' in between. Whereas at 40kHz and 60kHz, the reflections are less clear and the signals caused by the pulses of ultrasound circulating the chain becoming evident. The algorithm that is used to eliminate signals from pulses 'going the wrong' way through the rings starts to break down for certain wavelengths, and the circulating through-transmission pulses become superimposed on the pulse-echoes. At 50kHz, there was a lot of noise at the start of the trace. This is likely to be caused by the T(0,2) wave mode. Its cut-off is around 50kHz and therefore it is only excited at frequencies of 50kHz and above. However, around its cut-off frequency it will be highly dispersive which could cause this effect.

Finally, the model of the chain link was used to simulate a 50% cross sectional area flaw for the 10-cycle 30kHz case. The flaw was approximately 3mm wide at approximately 45 degrees. A-Scans showed a noticeable difference indicating that detection of the presence of the 50% cross sectional area of the flaw is possible.

2. Acoustic Emission approach

Structural integrity approaches have strongly recommended monitoring mooring chains insitu during operation to verify mooring integrity. To more accurately assess the operational condition of in-service mooring chains, it is beneficial to investigate the next-generation of monitoring technologies and their ability to detect flaws and corrosion prior to critical failure. One promising monitoring tool for providing early warning of flaws is Acoustic Emission (AE) testing, which has been used to successfully detect cracks in marine structures during operation.

Acoustic emissions are elastic waves that are spontaneously released by a material undergoing deformation. Acoustic emissions, or so-called 'hits' or events are the stress waves produced by the sudden internal stress redistribution of a material caused by changes in the internal structure. The stress can be hydrostatic, pneumatic, thermal, or bending. Possible causes of the internal structure changes are crack initiation and growth, crack opening and closure, dislocation movements. Materials emit ultrasound when they are stressed and fail on a microscopic scale (Huang, 1998).

The optimum AE parameters must be estimated for each application. The appropriate selection and installation of the AE sensors is crucial for a precise data collection strategy. The data must be processed to determine crack initiation and growth and to discriminate irrelevant information.

AE is used to detect defects in structures both in service and during manufacture. The technique can also be used to monitor defect growth during mechanical test in the laboratory. It is an ideal method for examining the behaviour of materials deforming under load.

The difference between an AE technique and other NDT methods is that the former detects active defects inside the material, while other the latter attempt to detect passive and active defects. Furthermore, AE needs only the input of one or more relatively small sensors on the surface of the structure or specimen being examined, so that the structure or specimen can be subjected to the in-service or laboratory operation, while the AE system continuously monitors the progressive damage.

The disadvantage of AE is that systems can only estimate qualitatively the extent of damage or size of defect. So, other NDT methods are still needed to do more exhaustive examination and provide quantitative results. Conventional ultrasonic evaluation is often used to evaluate AE indications. General guidelines for the preparation of your text

2.1. Finite element modelling

FEA has been used to analyse the AE wave propagation along the structure. As described in section 1.1, the model is linear elastic and assumed the following material properties for carbon steel: Young's modulus = 207GPa, Poisson's ratio = 0.3, Density = 7830kg/m3. A chain link of diameter 76mm was used in the analysis.

In the static analysis a model was run with a pressure of 1000Pa to find the equilibrium state. The force was applied on the region shown Fig. 4a which gave the result shown in Fig. 4b.

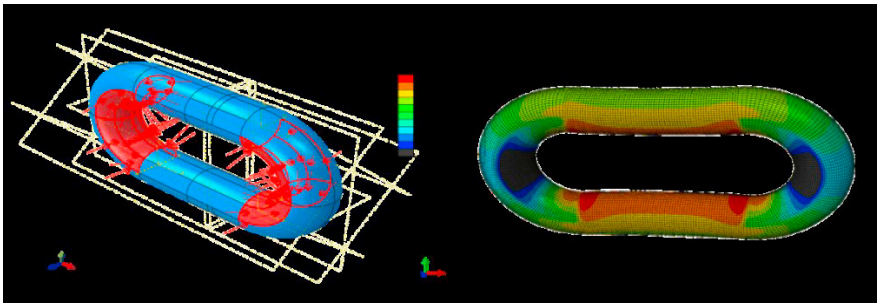

Fig. 4. (a) Area were force is applied; (b) distribution of stress along the chain.

In the dynamic analysis, the model of was created with the same geometry and same applied pressure, included a crack at the position indicated in Fig. 5. The shape was a segment of the circle, with maximum depth 10mm. The position was at the inner side of the join between curved section and straight section of the chain link.

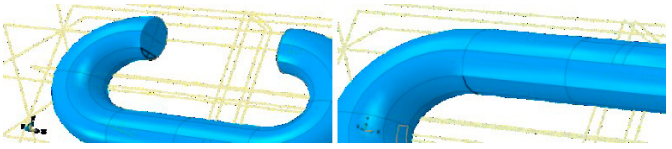

Fig. 5. Chain seam model view.

Two AE sensors were modelled in the dynamic model. Each was 10mm long, 29mm around the circumference, and positioned at 146.4mm along from the plane of the crack. They were positioned one at the top of the model (Sensor 1) and one at the bottom (Sensor 2) as shown in Fig. 6. The outputs were requested in the local cylindrical co-ordinate system (r, θ ,z).

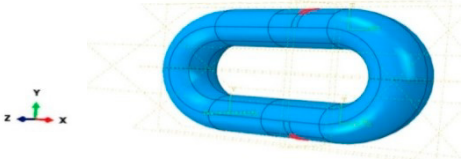

Fig. 6. AE sensors location: Sensor 1 top, Sensor 2 bottom.

Stresses from the static model were applied to the dynamic model as the initial conditions.

2.2. Modelling results

The dynamic model was solved in Abaqus for a simulated time of 0.5milliseconds. The crack opening can be observed in Fig. 7.

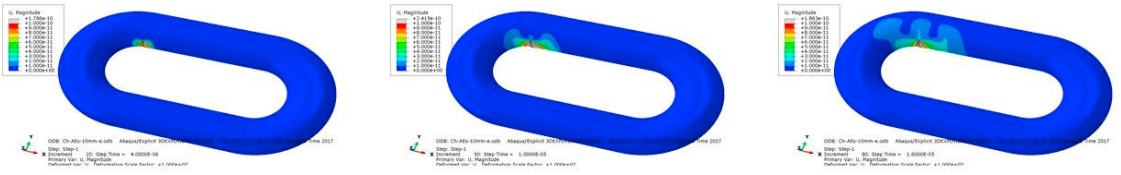

Fig. 7. Crack opening model.

The AE wave propagation and the displacement generated by the simulated crack growing can be observed in Fig. 8. This relates directly with the elastic waves released at the crack tip.

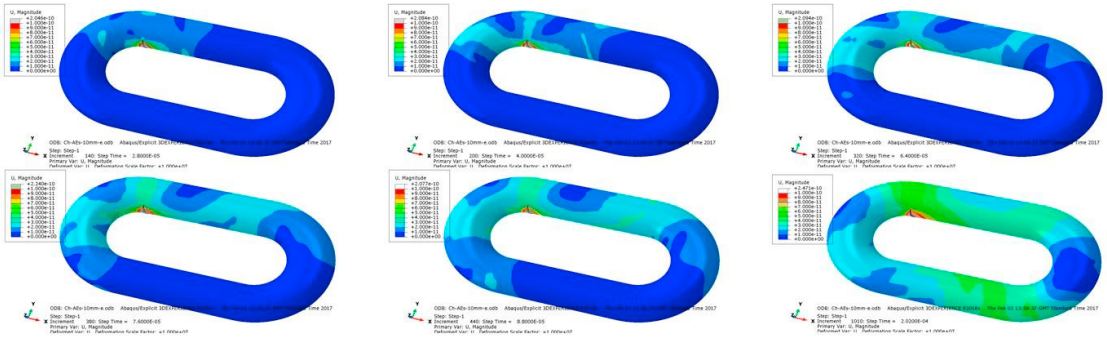

Fig. 8. Elastic waves propagation model.

The (r,θ,z) components of the displacements at each sensor location were recorded. Fig. 9 shows the displacement amplitude at both sensors location. The time of arrival (ToA) at each sensor can be observed. Calculating the value of the ToA, parameters such as the wave velocity or the location and time of occurrence can be estimated.

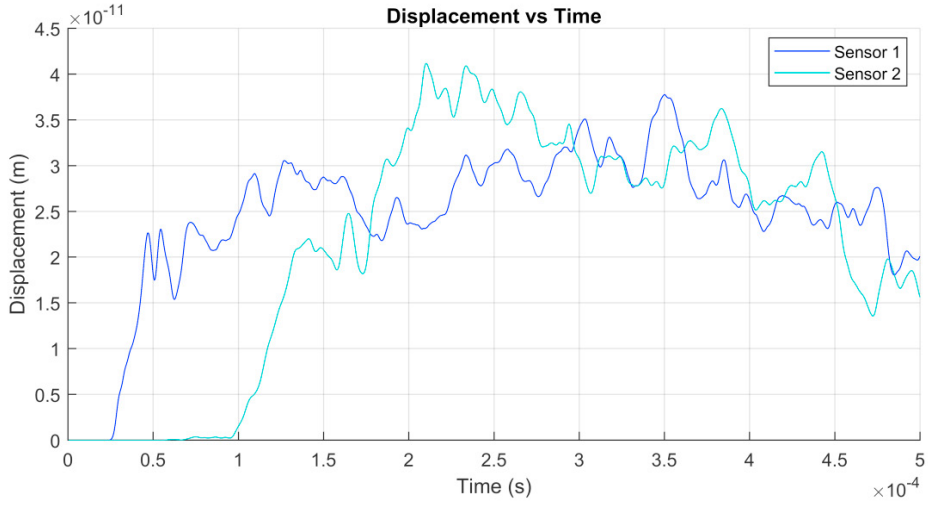

Fig. 9. AE waveform for S1 and S2: displacement module vs time.

The results of the elastic wave's propagation were treated as a model to test the method and to get the right definition. The mesh was made slightly finer although this had a very minor effect on the results. Two new cases were run for both 10mm and 1mm cracks with a finer mesh and a clearer definition.

The theoretical investigation of elasto-dynamic wave generation and propagation in mooring chains is the main interest of the present research. From the time and displacement representation, the propagation speed can be analysed. The model considers ideal conditions so the propagation is linear. Therefore there is no wave attenuation taken into account. Extrusion plots below represent a cross-sectional profile of the wave propagation along the chain link. The displacement is shown in relation with time. Fig. 10 presents the result of the AE wave propagating from the crack tip all around the link circumference. Different modes are generated when the waves propagate along the link surface. The horizontal axis shows the time in seconds, the vertical axis represents the link circumference in degrees and the colour scale represents magnitude of the displacement. The following results show the model when including the 10mm defect and an optimum mesh. Wave propagation is plotted along several link directions as shown in Fig. 10.

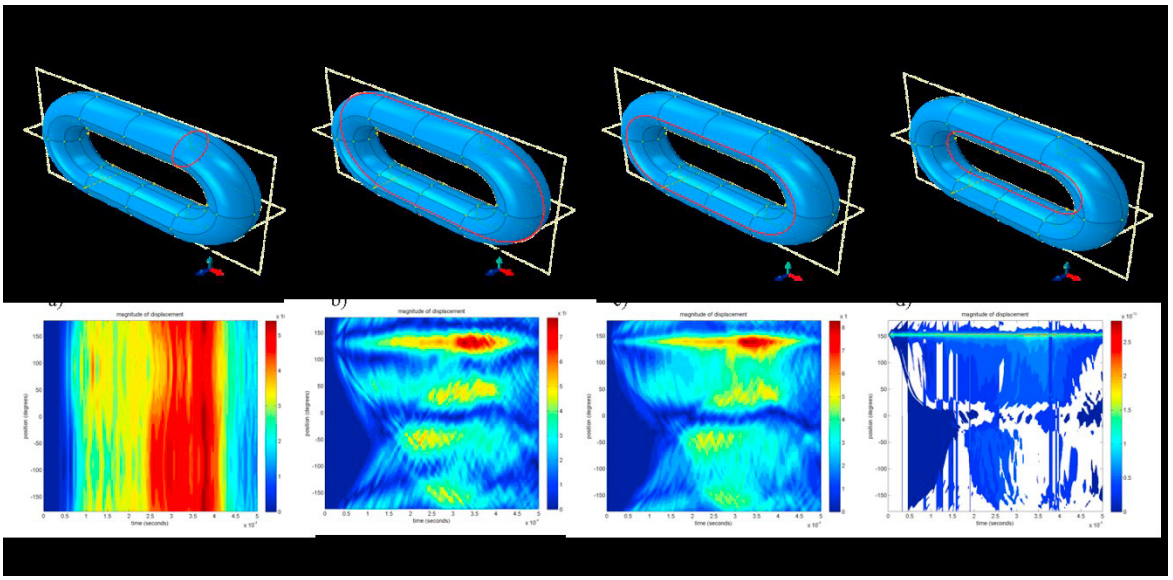

Fig. 10. Extrusion plots along several directions, 10mm crack depth; (a) around link circumference, (b) along outer circumference, (c) alongside circumference, (d) along inner circumference.

The ToA from the crack opening to the selected link circumference can be observed in Fig. 10a. As previously shown in Fig. 10 there is a period of time corresponding with zero displacement (blue) followed by the wave raise (yellow) in anticipation of the arrival of the wave's highest amplitude (red). Fig. 10b, Fig. 10c and Fig. 10d represent the displacement versus time at three different link circumferences. The crack position can be identified at approximately 149º where the wave amplitude can be observed to be higher. There is also a time dependency. The longest ToA occurs at around -50º, nearly 180º from the crack location.

The following results show the model with reduces crack size down to 1mm depth. Wave propagation is plotted along the link and the outer circumference as shown in Fig. 11.

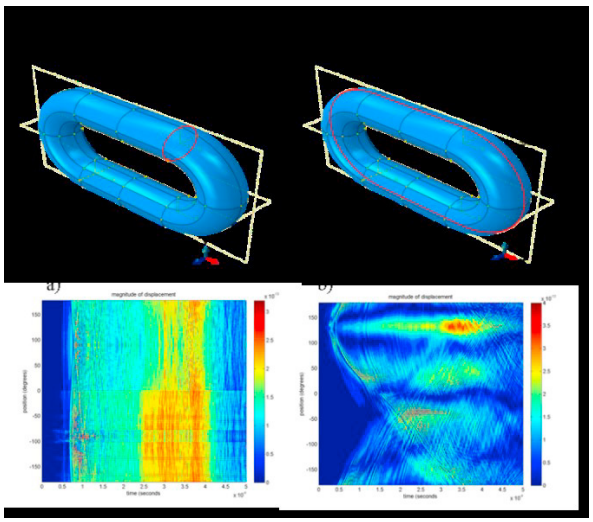

Fig. 11. Extrusion plots along several directions, 1mm crack depth; (a) around link circumference, (b) along outer circumference.

The maximum amplitude of the emissions generated by 1mm crack have decreased from the order of 10^{-11} to 10^{-13} in both (a) and (b) figures compared with the model using 10mm crack depth.

Fig. 11a shows again a period of time of no displacement (blue), an area of wave raising (yellow) and an interval where the wave highest amplitude is present (red). Fig. 11b illustrates the displacement at the crack position at nearly 149º where the wave amplitude can be observed to reach its highest.

Results in Fig. 12 show the wave propagation in terms of distance from the crack location. Not the same than the figures above, in this occasion the reference zero is located at the axial position of the defect. Positive distances are along the top straight section and right hand curve. Negative distances correspond to the left hand curve and then the bottom straight section.

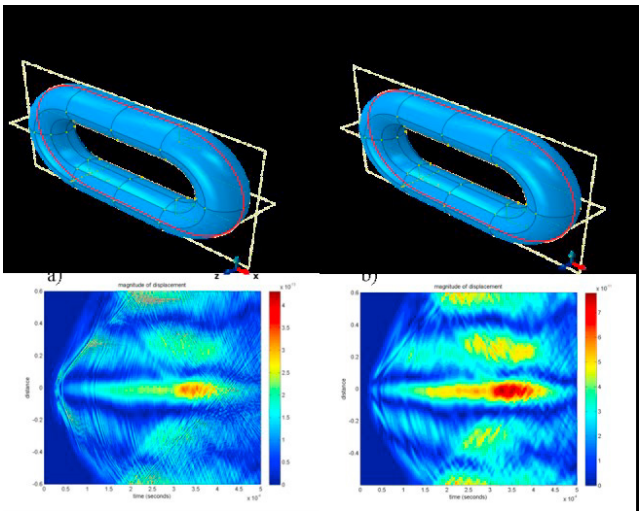

Fig. 12. Extrusion plots along outer circumference; (a) 1mm crack depth and (b) 10mm crack depth.

The maximum amplitude and wave energy of the AE waves generated at the 10mm crack tip have been proven to be 10^{-2} larger that the ones generated by the 1mm crack.

3. Final discussion

Due to the increasing demand of structural retrofit into conventional inspection strategies, SHM is of interest to an extensive range of industries. UGW and AE are non-destructive monitoring techniques which are widely employed at present. The output of its application will be comprehensive, real-time assessment of the structural condition of industrial assets.

The primary goal of this study was to investigate the applicability of UGW and AE approaches for crack initiation, location and propagation on a mooring chain. Modelling work has shown indication of the active damaged regions. Because of the inherent uncertainties present in any SHM technique, the described technologies should be applied as part of a full mooring chain structural integrity assessment. Recent developments in internet infrastructure and connectivity for monitoring and sensing present an opportunity to overcome the limitations of AE and UGW testing for continuous monitoring. In addition to the continuous data output, a risk-based Integrity Management strategy may also include, where available, data from periodic inspections, numerical modelling showing stress distributions or crack propagation, historic and current operations.

References

Thompson, D.O., Chimenti, D.E, 1996. Review of Progress in Quantitative Nondestructive Evaluation, Volumen 15. Twenty-second symposium on Quantitative Nondestructive Evaluation, 1995.

Desai, V. S., Pal, M., Banjare, M., Nancharaiah, C., Guria, S., & Vardhan, H., 2011. Use of long ultrasoinc testing (LRUT) technique for health assessment of critical piping in LPG service in a petroleum refinery.

Toigo, F., Marvin, A., Celli, V., & Hill, N. R. (1977). Optical properties of rough surfaces: general theory and the small roughness limit. Physical Review B, 15(12), 5618.

Sanderson, R., Smith. S., 2002. The application of finite element modelling to guided wave testing systems.

Huang, M., et al, 1998. Using acoustic emission in fatigue and fracture materials research. JOM 50.11: 1-14.

Sause, M. G., & Richler, S. (2015). Finite element modelling of cracks as acoustic emission sources. Journal of nondestructive evaluation, 34(1), 1-13.